Received Date : 27-Nov-2015

Revised Date : 31-May-2016

Accepted Date : 07-Jun-2016

Article type : Original Article - Platelets

Dynamics of calcium spiking, mitochondrial collapse and phosphatidylserine exposure in platelet subpopulations during activation

Sergey I. Obydennyy[*,†], Anastasia N. Sveshnikova[*,†,‡,‡], Fazly I. Ataullakhanov[*,†,‡], Mikhail A. Panteleev[*,†,‡,¶]

[*] Federal Research and Clinical Center of Pediatric Hematology, Oncology and Immunology, 1 Samory Mashela St, Moscow, Russia, 117198;

[†] Center for Theoretical Problems of Physicochemical Pharmacology, 4 Kosygina St., Moscow, Russia, 119991;

[‡] Faculty of Physics, Lomonosov Moscow State University, 1-2 Leninskiye Gory, Moscow, Russia, 119991;

[‡] Therapeutic Faculty, Pirogov Russian National Research Medical University, Ostrovitianova Str 1, Moscow, Russia, 117997

[¶] Department of Biological and Medical Physics, Moscow Institute of Physics and Technology, 9 Institutskiy per., Dolgoprudny, Moscow Region, Russia, 141700

Short title: Single-platelet procoagulant signaling

Corresponding author: Mikhail Panteleev, Federal Research and Clinical Center of Pediatric Hematology, Oncology and Immunology, 1 Samory Mashela St, Moscow, Russia, 117198, tel: +7-495-2876570 ext 6932; fax: +7-495-938-25-33; e-mail: mapanteleev@yandex.ru

Essentials

- The sequence and logic of events leading to procoagulant activity are poorly understood.
- Confocal time-lapse microscopy was used to investigate activation of single adherent platelets.
- Platelet transition to the procoagulant state followed cytosolic calcium oscillations.
- Mitochondria did not collapse simultaneously, and $\Delta\Psi$ loss could be reversible.

Abstract

Background. Activated platelets form two subpopulations, one able to efficiently aggregate, while another externalizes phosphatidylserine (PS) and thus accelerates membrane-dependent reactions of blood coagulation. The latter, procoagulant subpopulation is characterized by high cytosolic calcium and loss of inner mitochondrial membrane potential, and there are conflicting opinions on their roles in its formation.

Methods. We used confocal microscopy to investigate dynamics of subpopulation formation by imaging single, fibrinogen-bound platelets with individual mitochondria in them upon loading with calcium-sensitive and mitochondrial potential-sensitive dyes. Stimulation was with thrombin or protease-activated receptor 1 (PAR1) agonist SFLLRN. Stochastic simulations using computational systems biology model of PAR1 calcium signaling were employed for analysis.

Results. Platelet activation resulted in a series of cytosolic calcium spikes and mitochondrial calcium uptake in all platelets. Frequency of spikes decreased with time for SFLLRN stimulation, but remained high for a long period of time for thrombin. In some platelets, uptake of calcium by mitochondria led to the mitochondrial permeability transition pore opening and inner mitochondrial membrane potential loss that could be either reversible or irreversible. The latter resulted in cytosolic calcium rise and PS exposure. These platelets had higher cytosolic calcium before activation, and their mitochondria collapsed not simultaneously but one after another.

Conclusions. These results support a model of procoagulant subpopulation development following a series of stochastic cytosolic calcium spikes that are accumulated by mitochondria leading to a collapse, and suggest important roles of individual platelet reactivity and signal exchange between different mitochondria of a platelet.

Keywords: blood platelets, protease-activated receptors, calcium signaling, mitochondria, platelet activation

Abbreviations: PS, phosphatidylserine; PAR, protease-activated receptor; mPTP, mitochondria permeability transition pore; CypD, cyclophilin D; ADP, adenosine diphosphate

Introduction

Platelets are discoid cells 2-3 μm in diameter that circulate in blood at 200-300×10^3 cells/μl. Their main function is to prevent blood loss via two main mechanisms: i) formation of aggregates and ii) acceleration of the membrane-dependent reactions of blood coagulation by externalization of phosphatidylserine (PS) in the outer membrane leaflet and thus

providing binding sites for coagulation factors [1]; membrane-bound coagulation factors are additionally protected from blood flow [2]. In order to carry out these functions, platelets have to be activated, which can be done by a variety of agonists such as thrombin, collagen, ADP, etc. acting via numerous receptors (PAR1 and PAR4 for thrombin, glycoprotein VI for collagen, P2Y1 and P2Y12 for ADP, and so on [3, 4]). Although platelets are small and lack nuclei, their intrinsic organization is rather complex. They have dense tubular system, mitochondria, glycogen, numerous secretable granules, a contractable actin-myosin system, and an intricate signaling network to mediate and regulate their activation response [5]. Calcium signaling (Fig. 1A) is believed to be the central element of this network [4, 6].

One of the most interesting phenomena in platelet activation is that it results in the formation of at least two distinct subpopulations [7, 8], and that the two main platelet functions are unevenly distributed among them [9]. One subpopulation consists of living, amoeboid, well-aggregating platelets with no PS on their surface, while another (called "coated", "procoagulant", "necrotic" platelets [7-10]) includes balloon-shaped dead cells with externalized PS, a cap of alpha-granule proteins [11], excellent binding of coagulation factors [2, 12, 13], but no ability for independent aggregate formation [11, 14] and disrupted cytoskeleton disattached from adhesive receptors and thus additionally downregulating their adhesive properties [15].

Signal transduction mechanisms that define formation of these subpopulations are presently unclear. It is established that the subpopulations are not pre-existing [13, 14, 16]: the fraction of procoagulant platelets increases with the degree of activation, and can be easily changed between 0 and 90%. Experiments with various inhibitors, agonists, and patients with inherited platelet function defects allowed identification of the main receptors and signaling pathways [16-18], but not to determine the critical decision-making trigger mechanism that determines the future fate of a platelet. There is, however, evidence that this

trigger is somewhere in the cytosolic and mitochondrial calcium signaling. The non-procoagulant activated platelets seem to have low cytosolic calcium concentration, while the procoagulant subpopulation has high sustained cytosolic calcium [18, 19]. Single-cell calcium signaling has not been carefully compared between the subpopulations, though it is known that low-dose thrombin produces calcium spikes without significant PS externalization, while collagen surface induces stable calcium rise with PS [20]. Importantly, mPTP opening seems critically important to trigger the cell death processes leading to PS externalization in the procoagulant subpopulation [21], and importance of mitochondrial calcium sensor protein CypD suggests that this can occur as a result of mitochondrial calcium overloading [22]. However, there are conflicting opinions here, with some reports supporting importance of mitochondria but not cytosolic calcium as a decision-making unit [23], while others suggest it is cytosolic calcium that is important, and not mitochondria [24].

We recently used computational systems biology approach to propose a comprehensive picture of platelet subpopulation development; the model of calcium platelet signaling predicted that platelet stimulation via PAR1 produced cytosolic calcium spikes to become uptaken by mitochondria leading to their overload and mPTP opening in some platelets [25-27]; however, this picture still remains to be tested. The relationship between calcium dynamics, mitochondrial collapse and PS exposure in single platelets of different subpopulations has not been carefully elucidated experimentally and thus was the purpose of the present study.

Materials and methods

Reagents. The following materials were obtained from the sources shown in parentheses: human thrombin (Hematologic Technologies, Essex Junction, VT); prostaglandin E1 (MP Biochemicals, Irvine, CA); Fura Red AM, fluo-3 AM, rhod-2 AM, and

calcein-AM (Molecular Probes, Eugene, OR); Alexa Fluor 647-conjugated annexin V (Biolegend, San Diego, CA); PE-conjugated CD62P antibody (BD Biosciences, Franklin Lakes, New Jersey), tetramethylrhodamine methyl ester (TMRM) and nonyl acridine orange (NAO) (Life Technologies Grand Island, NY); cyclosporine A, calcium ionophore A23187 and CCCP (Tocris Biosciences, Bristol, UK). Integrin $\alpha_{IIb}\beta_3$ antagonist monafram [28] was a kind gift of Prof. A.V. Mazurov. All other reagents were from Sigma-Aldrich (San Diego, CA).

Blood collection and platelet isolation. Washed gel-filtered platelets were prepared essentially as described [11, 13, 14, 16, 18]. Briefly, blood was collected into sodium citrate and supplemented by apyrase (0.1 U/mL) and prostaglandin E1 (1 μmol/L). Investigations were performed in accordance with the Declaration of Helsinki, and written informed consent was obtained from donors. Platelet-rich plasma was obtained by centrifugation at 100 g for 8 minutes. Three parts of platelet-rich plasma were diluted with one part 3.8% sodium citrate (pH 5.5) and centrifuged at 400 g for 5 minutes, then platelets were resuspended in buffer A (150 mmol/L NaCl, 2.7 mmol/L KCl, 1 mmol/L $MgCl_2$, 0.4 mmol/L NaH_2PO_4, 20 mmol/L HEPES, 5 mmol/L glucose, 0.5% bovine serum albumin, pH 7.4) and gel-filtered on Sepharose CL-2B.

Confocal microscopy experiments: general design. Glass coverslips (24×24 mm, Heinz Herenz, Hamburg, Germany) were cleaned with potassium dichromate, rinsed with distilled water and dried. Then clean coverslips were covered with 1 mg/ml fibrinogen in distilled water for 45 min at room temperature, rinsed, and used as substrate for gel-filtered platelets. Platelets were spread on the fibrinogen-coated surface for 15 minutes, rinsed with buffer A with 2.5 mM $CaCl_2$ and video-imaging was started. Confocal images were acquired

using an Axio Observer Z1 microscope (Carl Zeiss, Jena, Germany) with a 1.3 NA 100x objective. Optical filters (Semrock Inc) for fluorophores were used: Alexa647-Annexin V, Fura Red (long pass filter 647+ nm); FITC-Annexin V, NAO (520/35 nm); TMRM, PE-CD62P (587/35). Excitation wavelengths were 488 nm for Fura Red, FITC, NAO, PE; 561 nm for TMRM; 635 nm for Alexa-647. Analysis of obtained images was carried out with ImageJ (http://imagej.nih.gov/ij/) software. Every single cell from field of view was traced along the contour and fluorescence (integral or mean for pixel of cell) for each dye for every time point was plotted as function of time.

Cytosolic calcium signaling. Before gel-filtration, resuspended platelets were incubated with 10 μmol/L Fura Red/AM or 10 μmol/L fluo-3/AM for 45 minutes at room temperature in the presence of apyrase (0.1 U/mL) and prostaglandin E1 (1 μmol/L). The concentration of the calcium-sensitive dye solvent, dimethyl sulfoxide did not exceed 0.1%; additional controls confirmed that the vehicle did not affect the results and the loading procedure did not have any significant effect on the PS-positive platelet formation. Platelets were activated under the conditions specified in the figures. Intracellular calcium levels were determined by confocal microscopy. Calcein was loaded to detect membrane integrity as described [29].

Detection of mitochondrial calcium entry and inner membrane potential. Rhod-2/AM was used as mitochondrial calcium indicator, TMRM was used to detect mitochondrial potential dynamics, and NAO was used to monitor integrity of mitochondria and control the mitochondrial specificity of TMRM labeling. Gel-filtered platelets were spread on the fibrinogen-coated coverslip for 15 minutes in presence of 5 μM Rhod-2 or 200 nM TMRM and/or 10 nM NAO at room temperature. Then unattached cells were removed with buffer A

with 2.5 mM $CaCl_2$ and imaging started as described above.

Statistics. Data are presented as means ± SD. The statistical significance of the differences between groups was determined by nonparametric Mann–Whitney U test. Differences were considered significant when $p<0.05$.

Computational modeling. For the starting predictions (section 3.1) a multicompartmental stochastic computational model of platelet calcium signaling resulting from stimulation of PAR1 receptor described in [25] was used. This Basic Model consisted of 27 ordinary differential equations and described reactions and species depicted in Fig. 1A. To explain observed in the current study experimental phenomena the Basic Model was elaborated into 2MitModel by addition of another distinct mitochondrion and including equations describing dependence of ATP production and calcium pumps activity on mitochondrial inner membrane potential. The 2MitModel consisted of 35 ordinary differential equations the corresponding reactions are listed in Table S1. The set of ordinary differential equation was solved using COPASI software (www.copasi.org), stochastic Adaptive SSA/tau-leap method.

Results

The Basic Model theoretical predictions. Stochastic computer simulations using the computational model of platelet's calcium signaling ([25], Basic Model) predicted several types of platelet response to PAR1 stimulation: i) calcium spiking with slowly decaying frequency, without significant mitochondrial calcium uptake and mPTP opening (Fig. 1B), ii) a more intense spiking with a reversible partial mPTP opening (Fig. 1C), and iii) intense spiking followed by an irreversible mPTP opening (Fig. 1D). In other words, calcium spiking

was the predominant mode of platelet response in the model, and procoagulant platelets were formed after a series of such spikes if they were sufficient to overload mitochondria with calcium. The model also predicted that individual platelet differences can pre-dispose them to becoming pro-coagulant [25], and that dependence of the spiking on the agonist concentration would be poorly discernible (Fig. S1). Noteworthy, because of strong non-linearity of the pore opening, slight differences in cytosolic calcium could determine whether the pore would open or not.

Dynamics of intracellular calcium and phosphatidylserine exposure. Fura Red-loaded platelets were used as a main tool to measure calcium dynamics in single cells, and fluo-3 was used as a control. Labeled annexin V was used to detect phosphatidylserine (PS) on the procoagulant "PS+" platelets (Fig. 2A, Supplement Video 1). Stimulation with an activator launched calcium signaling: Fura Red fluorescence immediately dropped down (as it is an inverse dye and its fluorescence decreases with calcium concentration increase), and prolonged frequent calcium oscillations were triggered that led some platelets to PS externalization (Fig. 2B-F). There were two distinct manners for a platelet to become "PS+": with prolonged oscillations (Fig. 2D) or rapidly, without clearly observed spiking (Fig. 2E). Unstimulated platelets showed occasional spikes, and there were no "PS+" platelets among them (Fig. S2C). Control experiments with a non-inverted fluo3 calcium dye confirmed observation of oscillations upon activation (Fig. S2E,F). As another control that decrease in Fura Red is not due to disrupted membrane integrity, we checked that platelets did not release calcein for at least 10 min after PS exposure under conditions of our study (Fig. S3A,B). Oscillations in the main body of the platelet and in the pseudopodia were the same (Fig. S3C).

The effect of the concentration and type of an activator on the platelet calcium response. We compared different concentrations of the activators and used two main agonists, PAR1 agonist SFLLRN and thrombin (that activates platelets via PAR1, PAR4, and probably via glycoprotein Ib-V-IX). Of these two, thrombin activation gave a more pronounced increase in the intracellular calcium than SFLLRN activation. Both SFLLRN (Fig. 3) and thrombin (Fig. 4) induced a rapid drop of Fura Red fluorescence upon activation. Calcium dynamics for same donor activated with SFLLRN (5 μM) and thrombin (50 nM) were different (Fig 4L, $p<0.001$). For SFLLRN, there usually were discernible spikes of calcium with slowly decreasing frequency; this agrees well with the expectations based on rapid PAR1 desensitization [25]. Thrombin always caused long-lasting oscillations. Noteworthy, in some cases transition of a platelet to the procoagulant state occurred just as a rapid calcum rise, without discernible spiking (Fig. 4G). The platelets that would not expose PS in all cases responded with calcium spiking of a widely varying degree for the whole duration of experiments. Proportion of PS+ platelet was linear across thrombin concentrations (Fig. S2B) and not for SFLLRN concentrations. That could be because of less percentage of "PS+" platelets in case of SFLLRN activation. "PS+" fraction was donor dependent. Stimulation of platelets with 10 μM of ionophore A23187 launched immediate loss of Fura Red intensity and exposure of PS in all platelets in field of view (Fig. S3D-G).

Correlation between Fura Red fluorescence in resting platelets before activation and PS exposure in the same platelets afterwards. To find out if there are PS-exposure-predisposing factors in platelets, we measured calcium in platelets before activation and compared obtained values for the platelets that had become "PS+" after experiment and for the platelets that were remaining "PS-" during 30 minutes. We grouped all the platelets into two subpopulations according to their PS exposure status at the end of the experiment (Fig.

5A). Then all platelets which exposed PS were combined in the "PS+" subpopulation and their average Fura Red fluorescences for every time point were plotted (Fig. 5B). These subpopulations had significant difference between Fura Red fluorescence for the period of time before the activation ($p<0.05$). Then the distribution was plotted for normalized fluorescence combining 11 experiments (181 "PS-" platelets and 55 "PS+"; different activators were used) and "PS+" subpopulation on the left part of distribution with a peak in 0.86 was found. "PS-" platelets had a peak at 1.00 (Fig. 5C, $p<0.001$).

Labeling of resting platelets for P-selectin revealed no detectable pre-activation and no correlation of the initial P-selectin value with PS exposure (Fig. S4A; compare with Fig. 2 where the same experiment is shown). This result was independent of the activator, both thrombin and SFLLRN gave the same result: "PS+" platelets had lower Fura Red fluorescence or higher intracellular calcium before activation (Fig. S4B,C).

To additionally check this observation and avoid artifacts of non-uniform labeling, we conducted experiments employing ratiometric technique. Fura Red was excited by 405 and 488 nm lasers and ratio of 405/488 intensities was calculated. Monafram was incubated with cover glasses prepared with plasma cleaner (Harrick Plasma) instead of fibrinogen. Activation with 100 nM of thrombin on the monafram surface provided same results that were obtained for fibrinogen surface. Platelets with higher initial calcium had more chances to exposure PS after stimulation (Fig. S4D, $p<0.01$)

Inner mitochondrial membrane potential dynamics during "PS+" subpopulation formation. We used potential-dependent fluorophore TMRM, which is accumulated in mitochondria, to monitor mitochondrial potential changes (Fig. 6A). Each "PS+" transformation was accompanied by a loss of mitochondrial potential and that process was almost simultaneous with cytosolic calcium increase and PS exposure (12 experiments with

74 “PS+” platelets; Fig. 6B-D). Interestingly, prior to the ultimate $\Delta\psi$ loss, there were occasions of temporary increase of whole-cell TMRM fluorescence (green arrows in Fig. 6B and D) that coincided with drops in TMRM fluorescence of single mitochondria (Fig. S5B-E). This is likely due to a temporary opening of mPTP in one or more mitochondria leading to TMRM exit and increase of its fluorescence; inside the mitochondria, the dye is less bright as a result of quenching that occurs at the concentrations employed here [30]. In agreement with that, addition of uncoupler CCCP caused a transient rise of TMRM fluorescence followed by a decrease later on (Fig. S5F). Ionophore A23187 affected in the same manner to TMRM fluorescence as CCCP addition (Fig. S3D-G). Furthermore, platelets that were pre-incubated with 5 μM cyclosporine A (CsA) had significantly lower “PS+” platelet fraction ($P<0.05$) in comparison with non-incubated platelets (Fig. 6G). While not new in itself [21, 22], this confirms the role of mPTP opening as one of the controlling steps in the PS exposure under conditions of this study.

Interestingly, mPTP opening was not simultaneous for different mitochondria of a same platelet. The potentials of different mitochondria from the same cell dropped one after another with delays of several seconds (Fig. 7A, Supplement Video 2). In some cells, mPTP opening in individual mitochondria was reversible without any PS exposure (Fig. 7B); very rarely, we observed irreversible loss of membrane potential in one mitochondria that did not spread to others (Fig. 7C). We used nonyl acridine orange (NAO, retained only in mitochondria, independent on membrane potential) loaded platelets to check if mitochondria were damaged during PS exposure (Fig. S6A,B). Platelets after 20 min of thrombin stimulation were imaged. All “PS+” platelets had significantly lower levels of NAO fluorescence (Fig. S6A) suggesting a high degree of mitochondrial damage. CsA did not essentially affect cytosolic calcium mobilization independently of mPTP opening (Fig. S6C-E).

Sequential mPTP opening in different mitochondria in computational model. To explain mechanics of the above described phenomena, namely cytosolic calcium rise after the mPTP opening and sequential collapse of distinct mitochondria, we expanded and modified the computational model. After the mitochondrial collapse, all calcium stored in the matrix goes into the cytoplasm. There it would be rapidly removed by the calcium ATPases (PMCA and SERCA). To prevent it we have included decrease in the ATPase activity due to the decrease in ATP level after mitochondrial collapse (Table S1) by a mechanism described in [31]. To describe sequential mitochondrial collapse phenomenon, we included another mitochondria in the computational model. The sequential collapse of two identical mitochondria in the *in silico* platelet is shown on Fig. 7D. The slight rise in cytosolic calcium concentration after collapse of the first mitochondrion leads to the increase in matrix free calcium concentration in the second mitochondria and followed by irreversible opening of mPTP in the second mitochondria. For mitochondria with different sizes the situation is similar: the collapse of the larger one leads to the collapse of the smaller one (Fig. S7A), and the collapse of the smaller one does not always lead to the collapse of the larger one (Fig. S7B). In line with the concepts discussed in this paper, addition of CCCP to activated platelets rapidly induced PS exposure (Fig. 7E).

Mitochondrial calcium dynamics during platelet activation. Fluorescent dye Rhod-2 was used to investigate calcium dynamics in mitochondria during platelet activation (Fig. 8). Rhod-2 distribution was compared in different fields of view before and after stimulation with 1 nM of thrombin to get rough estimates (Fig. 8A). Fluorescence of Rhod-2 became bright after stimulation, while non-activated cells had uniform emission. Overall low-time-resolution dynamics was obtained using low frequency of imaging (1 frame per 30 seconds) to avoid bleaching of the fluorophore (Fig. 8B) that clearly demonstrated

mitochondrial calcium increase after stimulation. Experiments with faster detection (1 frame per 2 seconds) and 5 μM SFFLLRN activation were able to show that alterations in Rhod-2 fluorescence in some spikes correlated with Fura Red signal: when Fura Red decreased, Rhod-2 signal was increased (Fig. 8D-E). Individual mitochondria correlated well in their calcium dynamics (Fig. 8D) and there was no discernible difference in mitochondrial calcium, which is not surprising taking into account great non-linearity of the mPTP opening (Fig. 1).

Discussion

The main result of the present paper is characterization of the signaling events occurring in individual cells of different platelet subpopulations after their physiological activation with thrombin or SFLLRN.

Although these subpopulations were known to differ in their cytosolic calcium concentration at some point after the activation [18, 19], those results were mostly obtained with flow cytometry and did not provide dynamics of cytosolic calcium changes in individual platelets. Some of the existing microscopy studies [20, 23] suggested that there should be spikes in the PS-negative platelets, but did not show it convincingly, and did not provide conclusive responses for the PS-positive ones. The classic paper [20] reported very frequent and blending spikes, but no PS exposure, upon thrombin stimulation; a more recent study [23] did not mention any spikes in either subpopulation, probably because most of the analysis used calcium signal integrated over many platelets. A previous computational study predicted that PS-positive platelets should appear after a series of spikes [25, 27], but only here we observed this experimentally (although there were some occasional platelets that exposed PS following just rapid cytosolic calcium rise without discernible oscillations in the present work). These results, together with the characterization of the activator-dependent

patterns of calcium spiking, provide a framework for further investigation and decyphering of platelet signaling responses.

The specific event responsible for triggering platelet death and PS exposure in a subpopulation of platelets has been for some time believed to be opening of mPTP [21, 22] likely resulting from mitochondria overloading with calcium [23] entering via a uniporter [25, 27]. The results on single-cell and single-mitochondria imaging obtained in the present study, including the effects of mPTP inhibition and observation of mitochondrial calcum increase (and leak once mPTP is opened), agree with such a mechanism. Yet they add some new information and demonstrate quite a new level of complexity. In agreement with theoretical predictions [25], mPTP opening is in many cases reversible. It also appears to be a stochastic phenomenon that does not occur simultaneously in all mitochondria of a platelet. Sometimes, mPTP can even open only in a single mitochondria while others retain their integrity for a long time. However, in most cases other mitochondria collapse relatively soon after the first one. The mechanisms responsible for this require additional reseach: it could be simply because their collapse is determined by the same history of cytosolic calcium, or because the first one releases calcium, or because the first mitochondrion stops to support ATP production and begins to destroy ATP instead. It is also interesting that, in agreement with model predictions, calcium levels in the mitochondria of procoagulant-platelets-to be do not differ greatly from those in the mitochondria of platelets that would not become procoagulant. This agrees well with previous hypothesis that non-linearity of pore opening is crucial to triggering the PS exposure [25, 27].

It has long remained a mystery whether there is some difference in platelets that predisposes some of them to becoming procoagulant. An early study of Alberio et al. suggested that platelet age might be important for development of procoagulant activity [32]. Ramstrom et al. elegantly demonstrated importance of PAR receptor density on the platelet

surface for platelet responses [33], but there was no PS exposure analysis in that study. In the present study, pre-activation cytosolic calcium concentration was different in future non-procoagulant and procoagulant platelets. Additional research is required to elucidate molecular mechanisms of this.

There are conflicting reports on the relative roles of cytosolic calcium and mitochondrial depolarization in the platelet subpopulation formation [21-24]. In our experiments, the causal and temporal consequence seems to be the following: i) formation of cytosolic calcium spikes upon agonist addition; ii) uptake of cytosolic spikes and increase of mitochondrial calcium with reversible $\Delta\Psi$ loss and, likely, mPTP opening in many cases; iii) irreversible mPTP opening in some of the cells; iv) high cytosolic calcium; v) PS exposure. The last three events are tightly interwoven, and all three develop simultaneously to a degree. Still, interestingly, mitochondrial collapse does not occur simultaneously in all mitochondria but rather spreads across the cell, and only once all are off PS is exposed. In contrast to [24], CsA did not essentially affect cytosolic calcium mobilization independently of mPTP opening, probably because we used SFLLRN, and not thapsigargin. In summary, the data of the present study support a unifying picture suggested in our theoretical study [25], where cytosol and mitochondria are both involved and are both important: cytosolic calcium spikes are accumulated by mitochondria and cause mPTP opening as a result of overloading. In addition to this, several unexpected findings appeared: a) difference of the baseline calcium concentration in the resting platelets as indicator of their tendency to become procoagulant, b) non-simultaneous loss of mitochondrial membrane potential raising questions about interactions between mitochondria, c) a wider range of the cytosolic calcium rise patterns observed experimentally. These data suggest new lines of theoretical and experimental research.

Conclusions

Stimulation of platelets using thrombin of PAR1 agonist SFLLRN initially produces a series of stochastic cytosolic calcium spikes. Their frequency decays with time for SFLLRN, and remains high for thrombin. Some platelets remain in this state. In others, there is a transition from spikes to sustained high calcium, because uptake of cytosolic calcium spikes by mitochondria leads to its overloading, mPTP opening, and PS externalization. Procoagulant platelets have higher cytosolic calcium in the resting state than non-procoagulant ones. $\Delta\Psi$ loss can be reversible. When irreversible, mitochondrial collapse does not occur simultaneously in all mitochondria but rather spreads across the cell.

Addendum

S. I. Obydennyy designed and performed experiments, analyzed the data and wrote the paper; A. N. Sveshnikova planned research, developed the model, performed simulations, designed experiments and analyzed the data; F. I. Ataullakhanov supervised the project and analyzed the data; M. A. Panteleev planned development and research, analyzed the data, wrote and edited the paper.

The authors declare that they have no conflict of interest.

Acknowledgements

We thank Prof. A.V. Mazurov for generously providing monafram. The study was supported by the Russian Science Foundation grant 14-14-00195. The funding agency had no involvement in either study design, or collection, analysis and interpretation of data, or in the writing of the report, or in the decision to submit the article for publication.

References

1. Zwaal RF, Comfurius P, Bevers EM. Surface exposure of phosphatidylserine in pathological cells. Cell Mol Life Sci 2005;62:971-88.

2. Podoplelova NA, Sveshnikova AN, Kurasawa JH, Sarafanov AG, Chambost H, Vasil'ev SA, Demina IA, Ataullakhanov FI, Alessi MC, Panteleev MA. Hysteresis-like binding of coagulation factors X/Xa to procoagulant activated platelets and phospholipids results from multistep association and membrane-dependent multimerization. Biochim Biophys Acta 2016;1858:1216-27.

3. Li Z, Delaney MK, O'Brien KA, Du X. Signaling during platelet adhesion and activation. Arterioscler Thromb Vasc Biol 2010;30:2341-9.

4. Lenoci L, Duvernay M, Satchell S, DiBenedetto E, Hamm HE. Mathematical model of PAR1-mediated activation of human platelets. Mol Biosyst 2011;7:1129-37.

5. Stalker TJ, Newman DK, Ma P, Wannemacher KM, Brass LF. Platelet signaling. Handb Exp Pharmacol 2012:59-85.

6. Varga-Szabo D, Braun A, Nieswandt B. Calcium signaling in platelets. J Thromb Haemost 2009;7:1057-66.

7. Munnix IC, Cosemans JM, Auger JM, Heemskerk JW. Platelet response heterogeneity in thrombus formation. Thromb Haemost 2009;102:1149-56.

8. Dale GL. Coated-platelets: an emerging component of the procoagulant response. J Thromb Haemost 2005;3:2185-92.

9. Heemskerk JW, Mattheij NJ, Cosemans JM. Platelet-based coagulation: different populations, different functions. J Thromb Haemost 2013;11:2-16.

10. Jackson SP, Schoenwaelder SM. Procoagulant platelets: are they necrotic? Blood 2010;116:2011-8.

11. Abaeva AA, Canault M, Kotova YN, Obydennyy SI, Yakimenko AO, Podoplelova NA, Kolyadko VN, Chambost H, Mazurov AV, Ataullakhanov FI, Nurden AT, Alessi MC, Panteleev MA. Procoagulant platelets form an alpha-granule protein-covered "cap" on their surface that promotes their attachment to aggregates. J Biol Chem 2013;288:29621-32.

12. Kempton CL, Hoffman M, Roberts HR, Monroe DM. Platelet heterogeneity: variation in coagulation complexes on platelet subpopulations. Arterioscler Thromb Vasc Biol 2005;25:861-6.

13. Panteleev MA, Ananyeva NM, Greco NJ, Ataullakhanov FI, Saenko EL. Two subpopulations of thrombin-activated platelets differ in their binding of the components of

the intrinsic factor X-activating complex. J Thromb Haemost 2005;3:2545-53.
14. Yakimenko AO, Verholomova FY, Kotova YN, Ataullakhanov FI, Panteleev MA. Identification of different proaggregatory abilities of activated platelet subpopulations. Biophys J 2012;102:2261-9.
15. Artemenko EO, Yakimenko AO, Pichugin AV, Ataullakhanov FI, Panteleev MA. Calpain-controlled detachment of major glycoproteins from the cytoskeleton regulates adhesive properties of activated phosphatidylserine-positive platelets. Biochem J 2016;473:435-48.
16. Kotova YN, Ataullakhanov FI, Panteleev MA. Formation of coated platelets is regulated by the dense granule secretion of adenosine 5'diphosphate acting via the P2Y12 receptor. J Thromb Haemost 2008;6:1603-5.
17. Ramstrom S, O'Neill S, Dunne E, Kenny D. Annexin V binding to platelets is agonist, time and temperature dependent. Platelets 2010;21:289-96.
18. Topalov NN, Kotova YN, Vasil'ev SA, Panteleev MA. Identification of signal transduction pathways involved in the formation of platelet subpopulations upon activation. Br J Haematol 2012;157:105-15.
19. London FS, Marcinkiewicz M, Walsh PN. PAR-1-stimulated factor IXa binding to a small platelet subpopulation requires a pronounced and sustained increase of cytoplasmic calcium. Biochemistry 2006;45:7289-98.
20. Heemskerk JW, Vuist WM, Feijge MA, Reutelingsperger CP, Lindhout T. Collagen but not fibrinogen surfaces induce bleb formation, exposure of phosphatidylserine, and procoagulant activity of adherent platelets: evidence for regulation by protein tyrosine kinase-dependent Ca2+ responses. Blood 1997;90:2615-25.
21. Remenyi G, Szasz R, Friese P, Dale GL. Role of mitochondrial permeability transition pore in coated-platelet formation. Arterioscler Thromb Vasc Biol 2005;25:467-71.
22. Jobe SM, Wilson KM, Leo L, Raimondi A, Molkentin JD, Lentz SR, Di Paola J. Critical role for the mitochondrial permeability transition pore and cyclophilin D in platelet activation and thrombosis. Blood 2008;111:1257-65.
23. Choo HJ, Saafir TB, Mkumba L, Wagner MB, Jobe SM. Mitochondrial calcium and reactive oxygen species regulate agonist-initiated platelet phosphatidylserine exposure. Arterioscler Thromb Vasc Biol 2012;32:2946-55.
24. Arachiche A, Kerbiriou-Nabias D, Garcin I, Letellier T, Dachary-Prigent J. Rapid procoagulant phosphatidylserine exposure relies on high cytosolic calcium rather than on mitochondrial depolarization. Arterioscler Thromb Vasc Biol 2009;29:1883-9.

25. Sveshnikova AN, Ataullakhanov FI, Panteleev MA. Compartmentalized calcium signaling triggers subpopulation formation upon platelet activation through PAR1. Mol Biosyst 2015;11:1052-60.
26. Balabin FA, Sveshnikova AN. Computational biology analysis of platelet signaling reveals roles of feedbacks through phospholipase C and inositol 1,4,5-trisphosphate 3-kinase in controlling amplitude and duration of calcium oscillations. Math Biosci 2016;276:67-74.
27. Shakhidzhanov SS, Shaturny VI, Panteleev MA, Sveshnikova AN. Modulation and pre-amplification of PAR1 signaling by ADP acting via the P2Y12 receptor during platelet subpopulation formation. Biochim Biophys Acta 2015;1850:2518-29.
28. Mazurov AV, Pevzner DV, Antonova OA, Byzova TV, Khaspekova SG, Semenov AV, Vlasik TN, Samko AN, Staroverov, II, Ruda MY. Safety, inhibition of platelet aggregation and pharmacokinetics of Fab'2 fragments of the anti-glycoprotein IIb-IIIa monoclonal antibody FRaMon in high-risk coronary angioplasty. Platelets 2002;13:465-77.
29. Topalov NN, Yakimenko AO, Canault M, Artemenko EO, Zakharova NV, Abaeva AA, Loosveld M, Ataullakhanov FI, Nurden AT, Alessi MC, Panteleev MA. Two types of procoagulant platelets are formed upon physiological activation and are controlled by integrin alpha(IIb)beta(3). Arterioscler Thromb Vasc Biol 2012;32:2475-83.
30. Perry SW, Norman JP, Barbieri J, Brown EB, Gelbard HA. Mitochondrial membrane potential probes and the proton gradient: a practical usage guide. Biotechniques 2011;50:98-115.
31. Magnus G, Keizer J. Model of beta-cell mitochondrial calcium handling and electrical activity. I. Cytoplasmic variables. Am J Physiol 1998;274:C1158-73.
32. Alberio L, Safa O, Clemetson KJ, Esmon CT, Dale GL. Surface expression and functional characterization of alpha-granule factor V in human platelets: effects of ionophore A23187, thrombin, collagen, and convulxin. Blood 2000;95:1694-702.
33. Ramstrom S, Oberg KV, Akerstrom F, Enstrom C, Lindahl TL. Platelet PAR1 receptor density--correlation to platelet activation response and changes in exposure after platelet activation. Thromb Res 2008;121:681-8.

Figure Legends

Figure 1. Possible modes of platelet calcium signaling. **(A)** The calcium signaling network in platelets. **(B-D)** Typical responses induced by 1-100 μM SFLLRN obtained as stochastic solutions of the computational model in individual platelets. (B) Calcum spiking with slowly decaying frequency, no calcium accumulation, no mPTP opening, 1 μM SFLLRN. (C) A more intense spiking with reversible partial mPTP opening, 10 μM SFLLRN. (D) Intense spiking followed by irreversible mPTP opening, 100 μM SFLLRN.

Figure 2. Experimental dynamics of intracellular calcium oscillations and PS externalization for different platelet subpopulations. **(A)** Images of Fura Red (calcium) and annexin V (PS) fluorescence. DIC images illustrated spreading platelets on the fibrinogen-coated surface before and after activation. Notations: “t start” – time of the start of the experiment; “t activation” – time of thrombin addition; ‘t 25 min” – 25 minutes after the start of the experiment. Scale bar equals 10 μm. **(B-E)** Fura Red (note that low fluorescence means high calcium concentration) fluorescence from single platelets on the fibrinogen-coated surface during 100 nM thrombin activation. Panels B and C show “PS-negative" cells, D and E are “PS-positive” cells. Panels A and B show “PS-negative" cells, C and D show “PS-positive” cells. Sustained high calcium level is indicated by red arrows. Plots are representative of a total of 80 “PS+” and 260 “PS-” platelets observed in 21 experiments. **(F)** Normalized Fura Red intensity for 20 “PS-negative” and 3 "PS-positive" platelets in a typical experiment. Means ± SD are shown. The difference between calcium levels immediately after activation was not very significant (170-270 seconds, $p\sim0.17$), while it was significant after PS exposure (900-1000 seconds, $p<0.001$).

Figure 3. Variability and concentration-dependence of platelet response to PAR1 activator. The panels show dynamics of calcium response and PS externalization in platelets that become either non-procoagulant **(A-D)** or procoagulant **(E)**. Conditions are as in Fig. 2, activation is indicated in the panels. SFLLRN caused frequent long-lasting calcium spikes or oscillations decaying with time. **(F)** Normalized Fura Red intensity for 30 "PS-negative" platelets activated with 5 μM SFLLRN and for 19 "PS-negative" platelets activated with 50 μM SFLLRN. Means ± SD are shown, the difference is significant ($p<0.01$).

Figure 4. Variability of platelet signaling upon activation by thrombin at different concentrations. The panels show dynamics of calcium response and PS externalization in platelets that become either non-procoagulant **(A-D)** or procoagulant **(E-J)**. Conditions are as in Fig. 2,3, apart that activation was with thrombin at 0.1 (A, E), 1 (B, F, G), 10 (C,H) or 50 (D, I, J) nM. (**G, I, J**) "PS+" platelets without long-lasting oscillations. **(K)** Normalized Fura Red intensity from 14 "PS-" platelets activated with 0.1 nM of thrombin, 20 cells with 1 nM, 23 cells with 10 nM and 21 cells with 50 nM of thrombin. Means ± SD are shown, $p\sim0.55$ for 0.1 nM versus 1 nM; $p< 0.05$ for 1 nM versus 10 nM. **(L)** Normalized Fura Red intensity from 19 "PS-" activated with 50 nM of thrombin and 10 cells activated with 5 μM of SFLLRN. Means ± SD are shown, $p<0.001$. Significance was measured between mean normalized Fura Red intensity of platelets in different experiments during 100 seconds after 50 seconds since the moment of activation.

Figure 5. Role of the pre-activation state. Platelets were activated in conditions described in Fig. 2. **(A)** Field of view before and in the end of video-imaging. Colors: green (Fura Red), red (annexin V). Activation was with 50 nM thrombin. Scale bar equals 10 μm. **(B)** Dynamics of Fura Red in different subpopulations before activation. Each single

spreaded platelet was allocated, specific fluorescences (integral intensity divided on square of the cell, with background substracted) of Fura Red were calculated, averaged for the same subpopulation and plotted for each time point ± SD. In this experiment, there were 19 "PS-" and 5 "PS+" cells. **(C)** Distribution of platelets with different Fura Red fluorescence prior to activation between subpopulations. The subpopulation state "PS+" or "PS-" for each cell was defined at the end of experiment (about 30 minutes after activation). There were 55 "PS+" and 181 "PS-" platelets from 11 experiments. The normalized values are integral cell fluorescences divided by cell area and then normalized on the average value for the PS- platelets in each experiment. Mean value for the normalized "PS+" subpopulation equaled 0.86 and 1 for "PS-" subpopulation ($p<0.001$). Lower fluorescence indicates higher calcium level.

Figure 6. Mitochondrial membrane potential dynamics of thrombin activated platelets. Platelets were loaded with Fura Red and TMRM. (**A**) Field of view before activation (first line) and after 800 seconds (second line). Blue is TMRM; green is Fura Red; red is a annexin V. Activation was with 50 nM thrombin. Scale bar equals 10 μm. **(B-E)** Dynamics of Fura Red, TMRM, annexin V for "PS+" platelets (**B-D**) and for "PS-" platelet (**E**). Decrease of mitochondrial membrane potential and Fura Red fluorescence are simultaneous with PS exposure. In some platelets coupled fluorescence bounces of TMRM and Fura Red were observed (green arrows). (**F**) Normalized Fura Red and TMRM intensities from 10 "PS-" platelets in the experiment. Mean ± SD. (**G**) Platelets were incubated with 5 μM CsA during spreading on the fibrinogen (15 minutes), washed with buffer plus 5 μM CsA and then activated with 10 nM thrombin plus 5 μM CsA in presence of labeled annexin V. After 15 minutes of activation, different fields of view were registered and fraction of "PS+" platelets were counted and compared between CsA treated and non-treated specimens. 4500 cells from

3 donors were observed. Every time CsA significantly reduced fraction of "PS+" platelets. Percentages of "PS+" platelets from 3 donors were averaged and plotted ± SD, $P<0.05$.

Figure 7. Mitochondria depolarization is not simultaneous and can occur in the "PS-" platelets. Platelets were loaded with TMRM (green) and activated with 5 μM SFLLRN in presence of annexin V (red). See also Supplement Video 2. **(A)** Short period of time before PS exposure demonstrated. White arrows indicate individual mitochondria that undergo collapse one after another. **(B-C)** Reversible and irreversible loss of mitochondrial membrane potential in "PS-" platelets respectively. Platelets **(B-C)** did not expose PS during all time of experiment (20 and 30 minutes). Time points indicated are relative to the first shown frames. Scale bar equals 1 μm. (D) Computational model "2MitModel": sequential mitochondria collapse. Two identical mitochondria with equal numbers of all components and volumes were simulated instead of one. Collapse of one mitochondrion leads to the $\Delta\psi$ loss, subsequent decrease in calcium pump activity and ATP concentration according to the mechanism described in [31]. This increases possibility of the second mitochondrion collapse. **(E)** Platelets were incubated with 10 μM CsA, and activated with 10 nM of thrombin. Addition of the CCCP after 820 seconds dropped mitochondrial potential and the percent of PS+ platelets was increased from 2% to 24% during 3 minutes after CCCP addition. The scale is 10 microns, annexin V is red and Fura Red is green.

Figure 8. Mitochondrial calcium dynamics of activated platelets. Platelets were loaded with 5 μM Rhod-2. **(A)** Rhod-2 distribution before and after 20 minutes of platelet activation with 1 nM of thrombin. Fluorescence was distributed uniformly in every cell before activation. At the end of experiment fluorescence in mitochondria were increased. **(B)** Dynamics of Rhod-2 fluorescence in 5 different "PS-" platelets. Frames were obtained every

30 seconds to prevent bleaching and determine overall dynamics. Fluorescence increased in every platelet after addition the activator that led to moderate growth of fluorescence. **(C)** Normalized Fura Red and rhod-2 intensity from 10 "PS-" platelets in the experiment. Mean +- SD. **(D-E)** Rhod-2 fluorescence dynamics in "PS-" and "PS+" platelets respectively. Spikes of Rhod-2 fluorescence correlate with Fura Red fluorescence decrease. Integral signals presented, noise substracted.

Figure 1

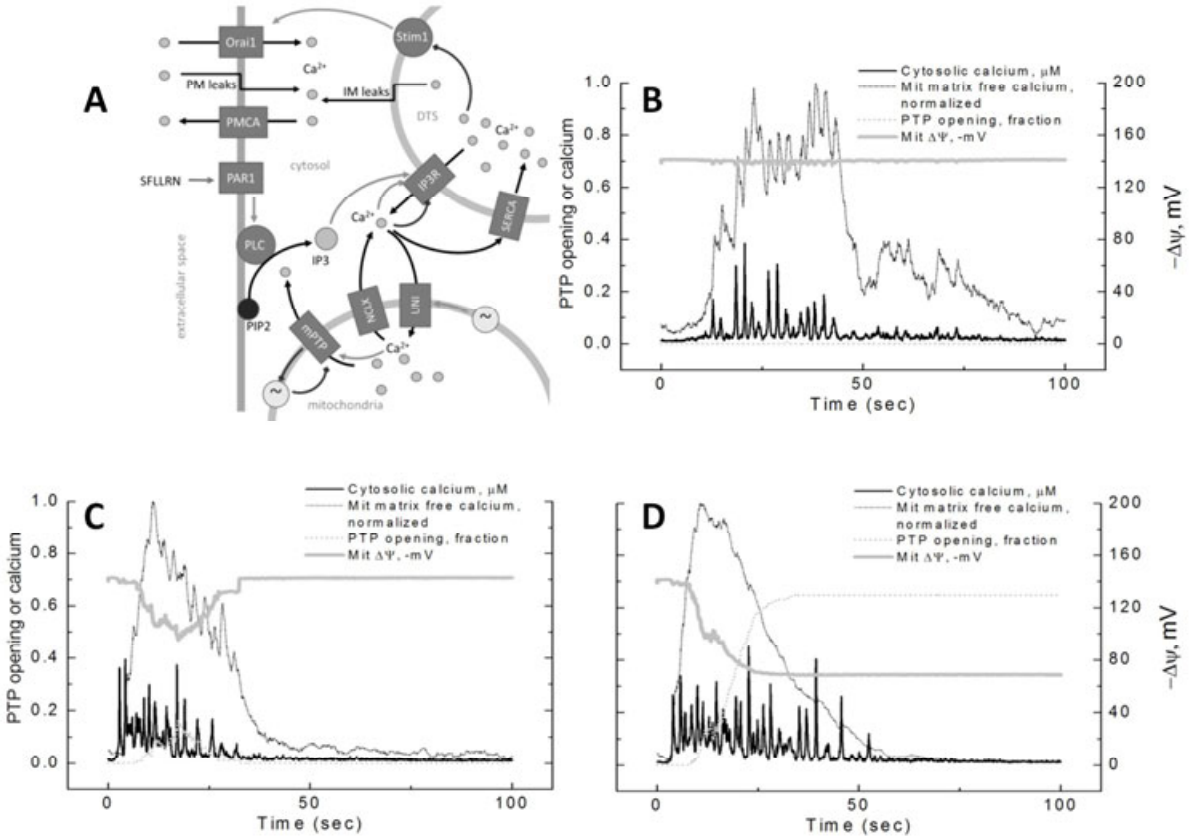

Figure 2

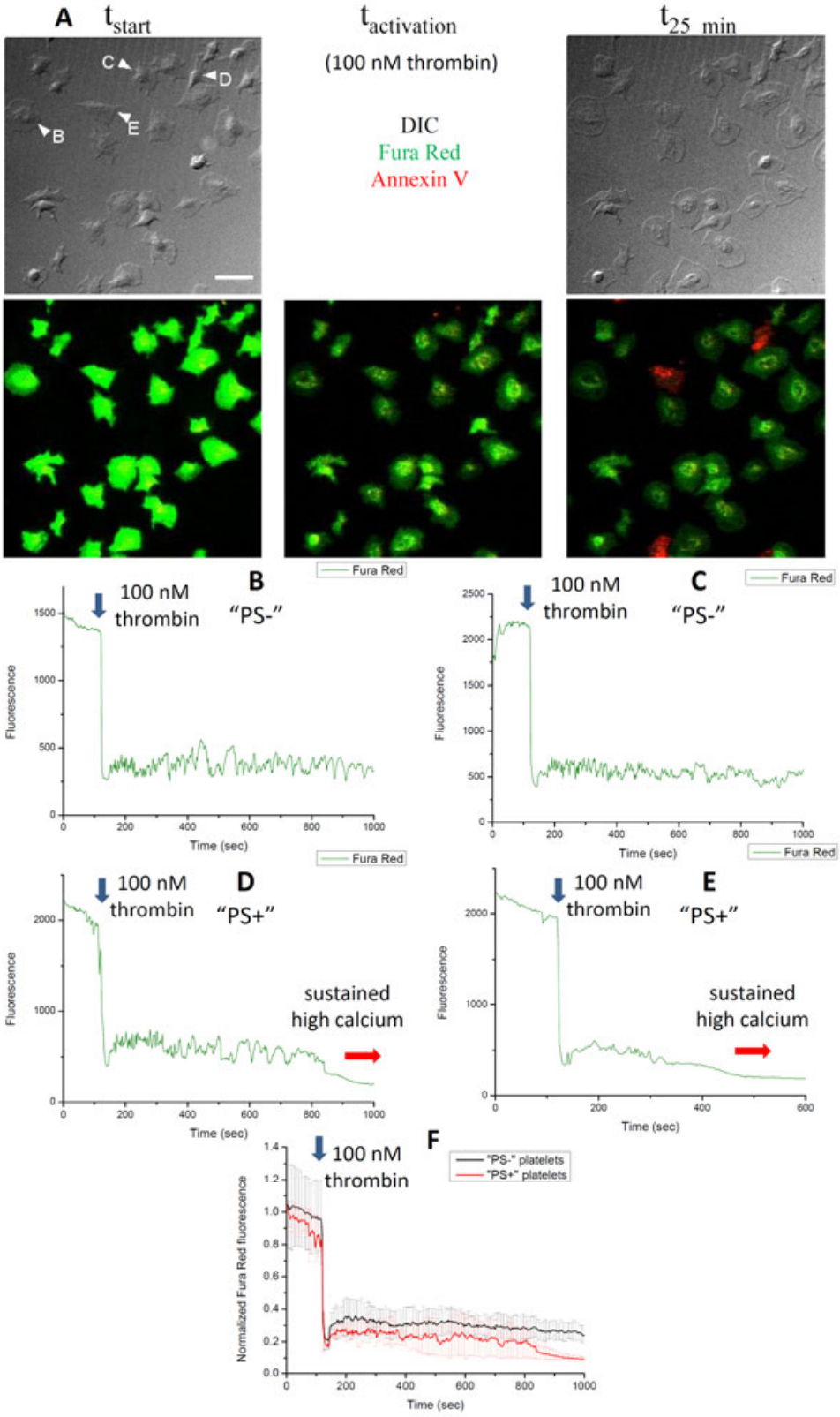

Figure 3

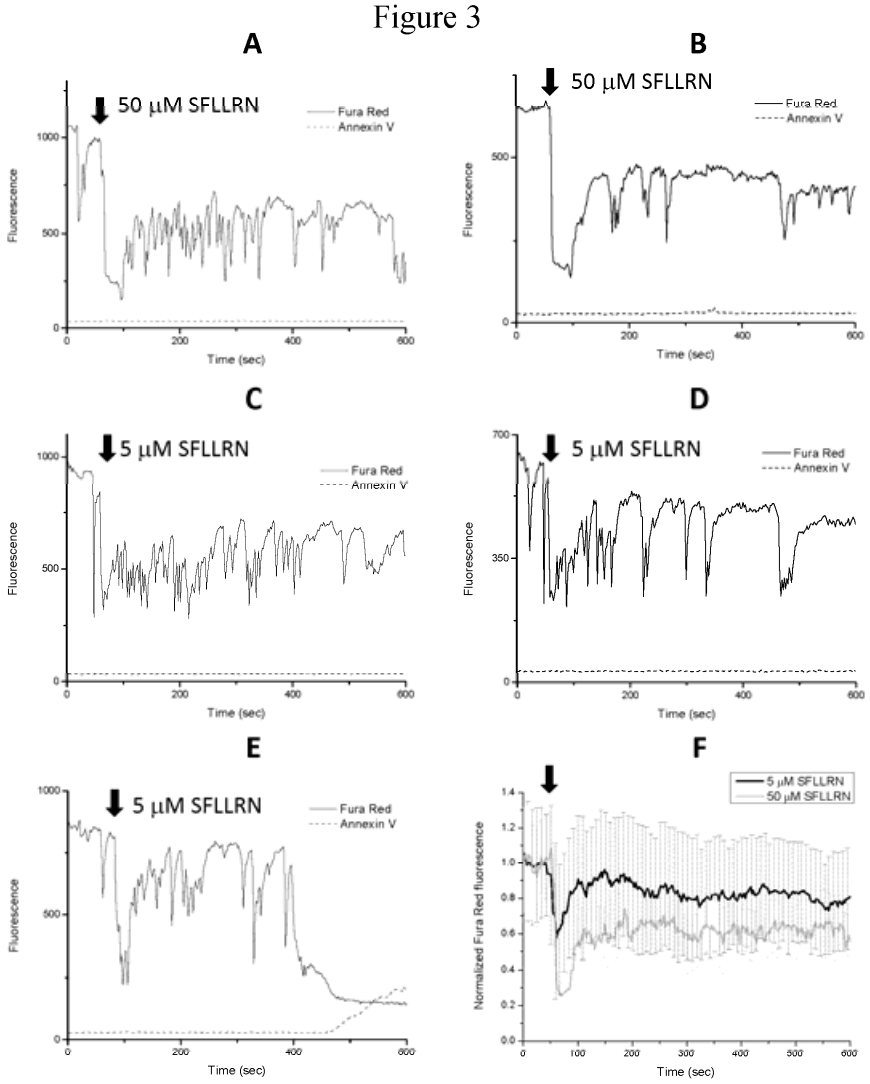

Figure 4

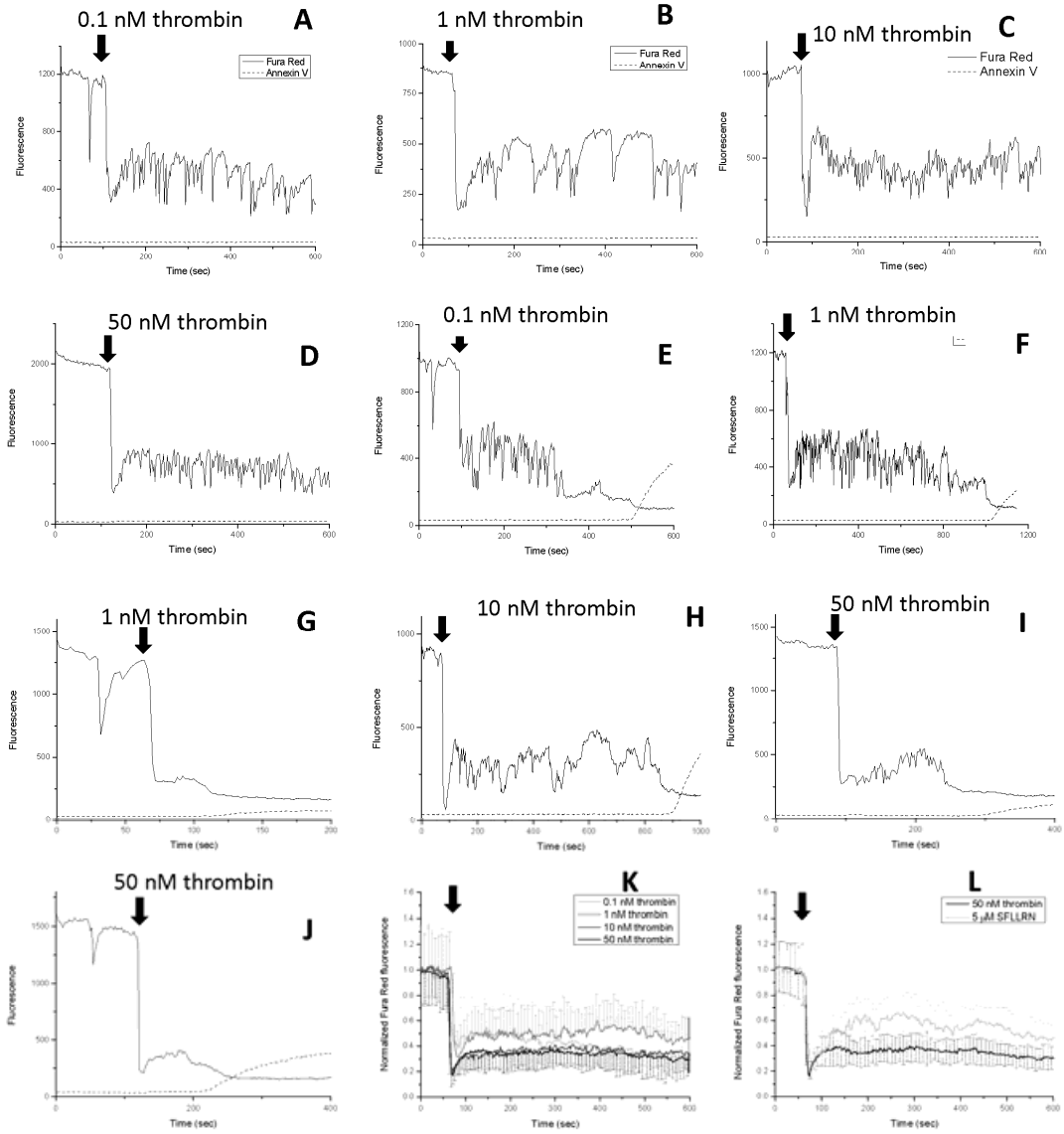

Figure 5

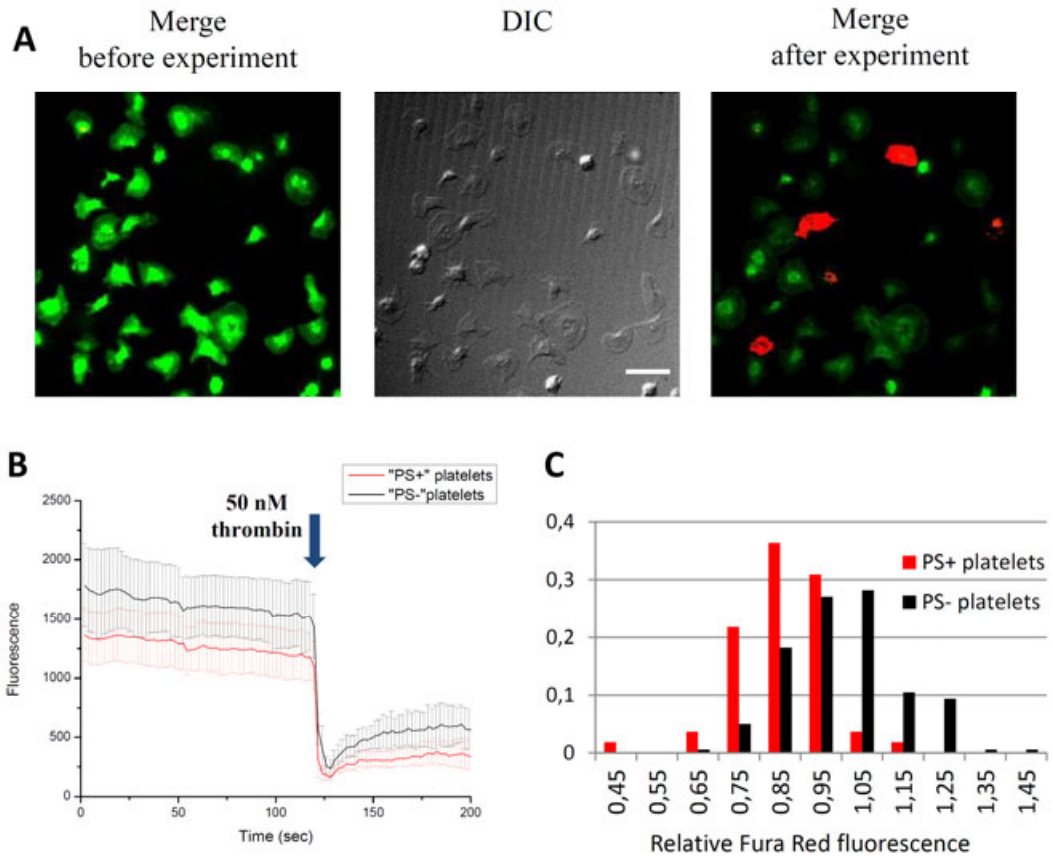

Figure 6

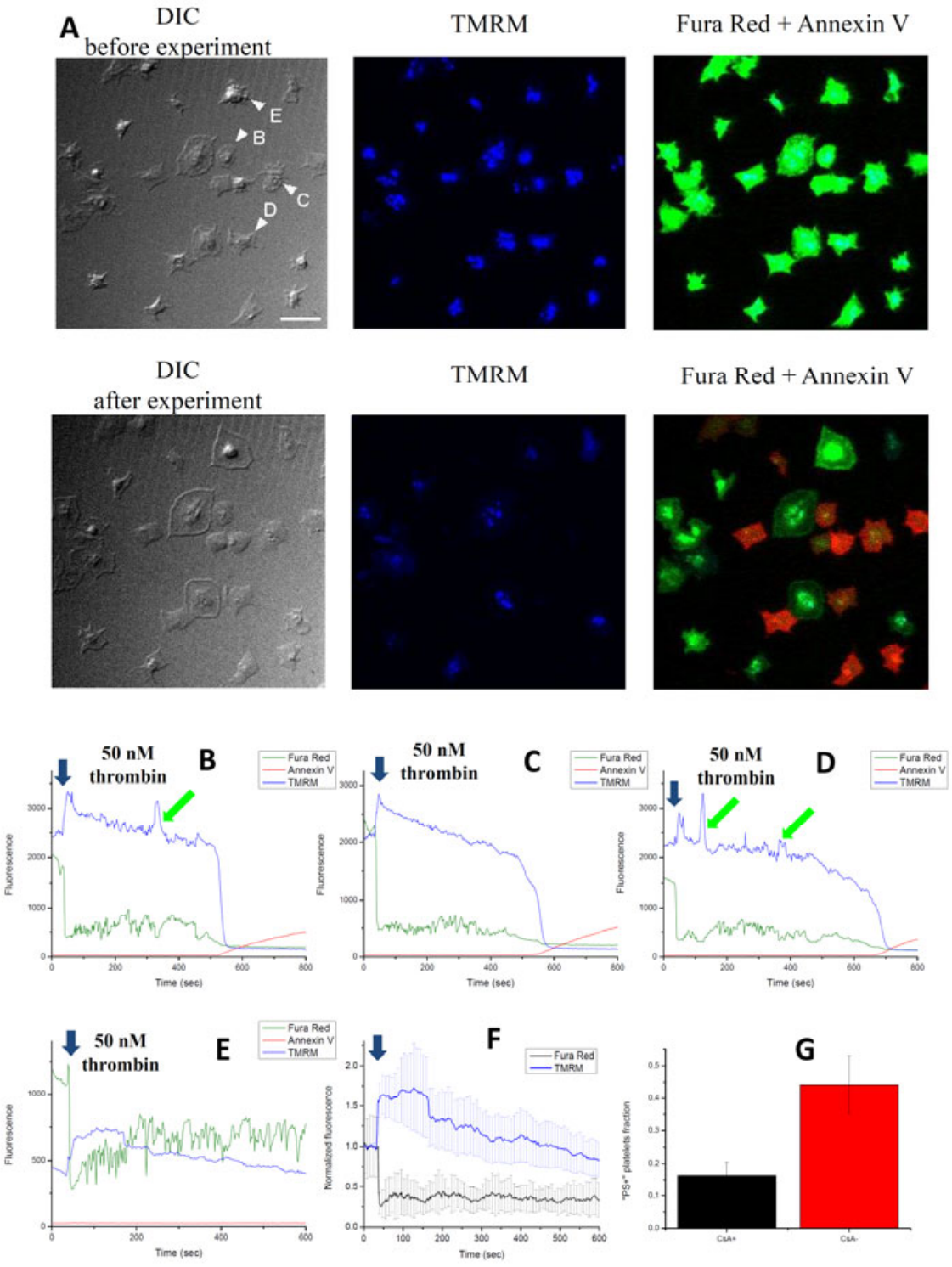

Figure 7

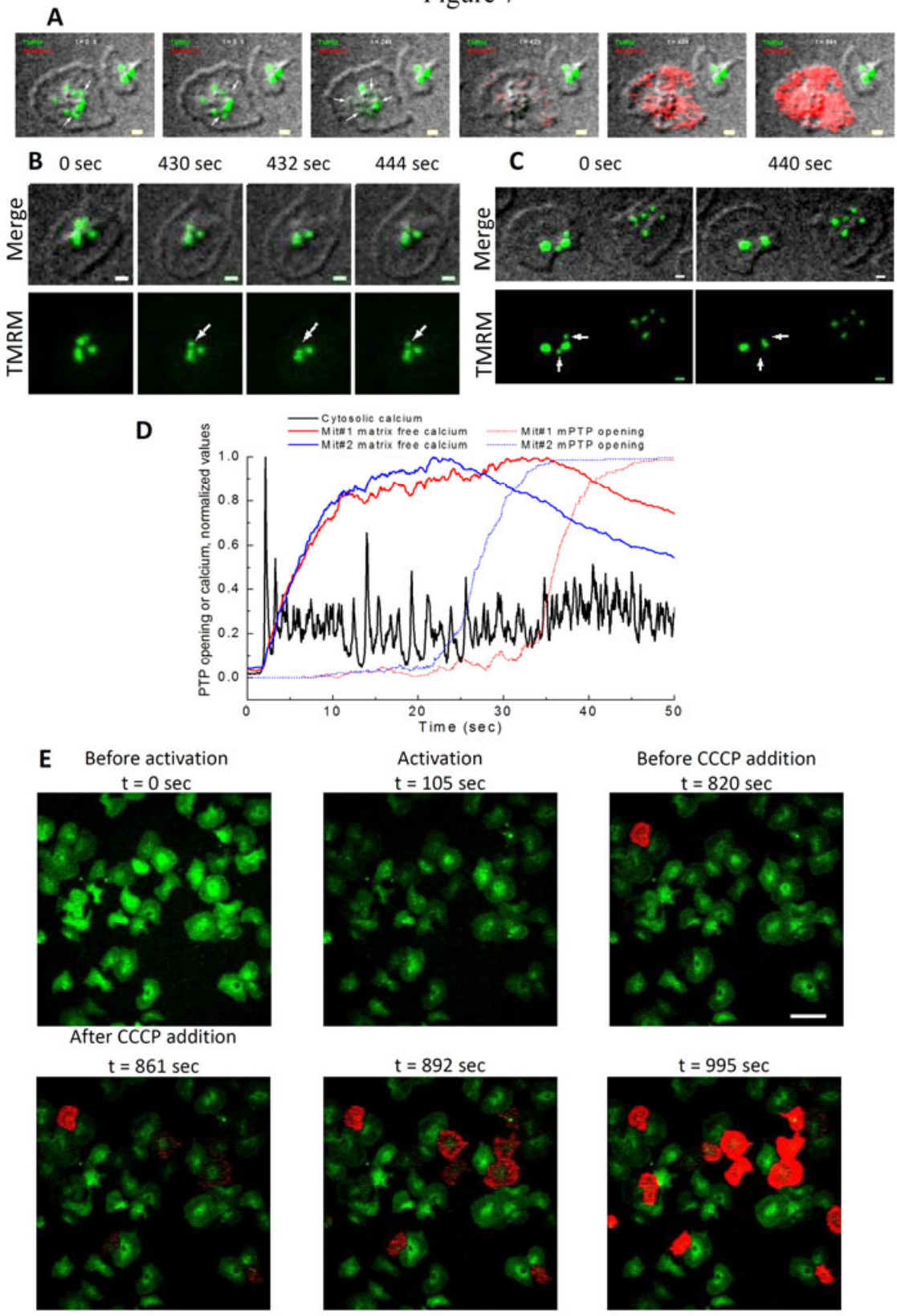

Figure 8